Food Research International 120 (2019) 449–455

Contents lists available at ScienceDirect

Food Research International

journal homepage: www.elsevier.com/locate/foodres

Analysis and modeling of enhanced green fluorescent protein diffusivity in whey protein gels

Qi Luo[a], Erik Sewalt[a], Jan Willem Borst[b,c], Adrie H. Westphal[b,c], Remko M. Boom[a], Anja E.M. Janssen[a,*]

[a] Food Process Engineering, Wageningen University, P.O. Box 17, 6700 AA, Wageningen, the Netherlands
[b] Laboratory of Biochemistry, Wageningen University, P.O. Box 8128, 6700, ET, Wageningen, the Netherlands
[c] Microspectroscopy Research Facility, Wageningen University, P.O. Box 8128, 6700, ET, Wageningen, the Netherlands

ARTICLE INFO

Keywords:
FCS
GFP
Pepsin
Whey protein gel
Diffusion
Modeling
Gastric digestion

ABSTRACT

During gastric digestion, hydrolysis of proteins by pepsin contributes largely to the breakdown of protein-rich food. We hypothesized that the effect of pepsin is limited by its diffusivity, which is co-determined by the food structure and the local pH in the food during digestion. To investigate the principle mechanism of enzyme diffusion in food matrices, we used enhanced green fluorescent protein (EGFP) as probe to study the diffusivity of proteins in whey protein isolate gels, using fluorescence correlation spectroscopy (FCS). Gels made with different ionic strength showed distinctive elastic moduli but did not show differences in diffusivity of EGFP. Some models for diffusion in hydrogels yield good description of the obtained data, and can approximate the enzyme diffusion in diverse food matrices. However, the enzyme pepsin is more complicated than the probe EGFP, to yield more accurate predictions, electrostatic and enzyme-substrate interaction also need to be considered.

1. Introduction

The digestion kinetics of food are dependent on the structure of the food that is digested. Food structure influences the oral processing, the gastric disintegration rate, and the consequent gastric emptying towards the duodenum (Singh, Ye, & Ferrua, 2015). The gastric disintegration of food invovles physical and chemical processes, including the peristalsis of the stomach, acid hydrolysis and enzymatic reactions (Bornhorst & Singh, 2014). Among these processes, hydrolysis of proteins by pepsin contributes largely to the breakdown of protein-rich food in the stomach. This hydrolysis can limited by the diffusion of pepsin and the local pH in the solid food matrix during digestion. The hydrolysis kinetics of egg white protein gels and whey protein gels differed strongly from that of the same proteins in solution, which is likely due to the diffusion limitation in gels for both the pepsin and the hydrolysates (Luo, Boom, & Janssen, 2015). Compared to acid-induced dairy gels, a rennet-induced casein gel consists of compact protein aggregates in the acidic gastric environment, and the rennet gel had much slower proteolysis kinetics than that of acid-induced gels (Floury et al., 2018). Thus, a quantitative investigation of pepsin diffusion in food structures may contribute to the understanding of food breakdown and digestion kinetics.

We previously measured the diffusivity of pepsin in whey protein isolate (WPI) gels by fluorescence correlation spectroscopy (FCS). We found that the pepsin does not penetrate deep into the gel but remains in a thin layer below the surface of the gel. A second finding was that the diffusivity of pepsin depends strongly on the concentration of the protein gels (Luo, Borst, Westphal, Boom, & Janssen, 2017). Fluorescence Correlation Spectroscopy (FCS) was used for its non-invasiveness and suitability to be used within protein gels. In FCS, a confocal laser microscope is coupled with a photon detector to measure fluorescence intensity fluctuations in a small focal volume. If these fluctuations originate primarily from the diffusion of the fluorophores through the focal volume, autocorrelation analysis can quantify the diffusion rate of the fluorophore.

Whey protein gels were used before as model for protein-based solid foods (Luo et al., 2017). Whey protein gelation is generally a two-step process. After heat denaturation, protein oligomers form primary aggregates with different shapes and sizes depending on the pH and the salt concentration. These primary aggregates then form large self-similar aggregates that precipitate or gel above a critical concentration (Aymard et al., 1996; Nicolai, Britten, & Schmitt, 2011). At neutral pH, the primary aggregates consist of short, curved strands with a length of about 50 nm and a diameter of about 10 nm, independent of ionic

* Corresponding author.
E-mail address: anja.janssen@wur.nl (A.E.M. Janssen).

https://doi.org/10.1016/j.foodres.2018.10.087
Received 10 April 2018; Received in revised form 28 October 2018; Accepted 30 October 2018
Available online 01 November 2018

strength. At low ionic strength, the large aggregates mainly form via head-to-tail association of the primary aggregates, while at higher ionic strengths the structure is more densely branched (Nicolai et al., 2011; Pouzot, Nicolai, Visschers, & Weijers, 2005).

We here aim to find an appropriate model to describe diffusion in protein gel matrices, for predicting pepsin diffusion in food during gastric digestion. We also explore the correlation between a macroscopic parameter such as the elastic modulus and the diffusivity of a protein in the gel. Two types of whey protein gel matrices were constructed by altering the ionic strength but keeping the same protein concentration, so that we can compare the diffusion in the gels at the same volume fraction but at different gel strengths. Enhanced Green Fluorescent Protein (EGFP) was used as the pepsin analogue since it has a similar size (The molecular weight of EGFP is 26.9 kDa and the unit cell dimensions of EGFP crystal are 5.1 nm × 6.3 nm × 7.1 nm (Ormo et al., 1996); the molecular weight of pepsin is 34.6 kDa and the unit cell dimensions of pepsin crystal are 5.5 nm × 3.6 nm × 7.4 nm (Sielecki, Fedorov, Boodhoo, Andreeva, & James, 1989)) and similar diffusivity to pepsin (Luo et al., 2017). EGFP is auto-fluorescent, thus it can avoid the possible interference of dissociated free dye from the conjugate. Thévenot, Cauty, Legland, Dupont, and Floury (2017) have quantified pepsin diffusion in dairy gels and applied models of polymer science to predict the diffusion coefficients. Quantification of enzyme diffusion in food products will not only improve the understanding of digestion, but may also elucidate the bioaccessibility of proteins and other nutrients. Moreover, the activity of pepsin inside a protein gel network can change the structure of the network, which may lead to a change of diffusivity (Luo et al., 2017). Models that account for such a change of structure during digestion can offer better descriptions of the diffusivity.

2. Theory

Many models for solute diffusion in hydrogels are based on the hydrodynamic theory or the obstruction theory (Amsden, 1998; Masaro & Zhu, 1999). The hydrodynamic theory is based on the Stokes-Einstein equation for solute diffusivity. The solute is assumed to be a hard sphere which moves with constant average velocity through a continuous solvent, experiencing friction. Polymer chains present in the medium reduce the local velocity of the fluid, and hence increase the friction of a solute with its surroundings. In the obstruction theory, the polymer chain network obstructs specific sites that were otherwise available for the solute, and therefore reduces the available paths for diffusion. The chains themselves are considered immobile and impenetrable for the solute. The models have been thoroughly discussed in the two reviews of Amsden (1998) and of Masaro and Zhu (1999). We selected some models based on their feasibility for our system of interest. One of the models is based on the hydrodynamic theory, some models on the obstruction theory and some models combine the theories. These models are briefly discussed hereafter, the meaning of each symbol is listed in Table 1.

Cukier's model (Eq. 1) is based on the hydrodynamic theory, and that assumes the friction of the solute with the medium is the main cause of reduced diffusion rate (Cukier, 1984):

$$\frac{D}{D_0} = exp(-k_c r_s \phi^{\nu}) \tag{1}$$

Ogston's model (Eq. 2), based on obstruction-scaling theory, assumed solute diffusion is a succession of directionally random unit steps (Ogston, Preston, & Wells, 1973). The polymers are considered to be long, straight fibers of small width, while the solute is considered as a hard sphere. The unit step was defined as the root-mean-square average diameter of the spherical solute molecules within the fiber network.

$$\frac{D}{D_0} = exp\left[-\frac{r_s + r_f}{r_f}\sqrt{\phi}\right] \tag{2}$$

Table 1
List of symbols.

Symbol	Description
D	Diffusion coefficient ($m^2 s^{-1}$)
D_0	Diffusion coefficient at infinite dilution ($m^2 s^{-1}$)
r_s	Radius of the solute (nm), calculated using the Stokes-Einstein equation: $r_s = \frac{k_B T}{6\pi\eta D}$. Where k_B is the Boltzmann's constant, T is temperature and η is the solvent viscosity.
r_f	Radius of the polymer fiber (nm)
ϕ	Polymer volume fraction $\phi = \nu \times C$, where v is the voluminosity (mL g^{-1}) and C is the mass concentration (g mL^{-1})
α	$\alpha = \phi\left(\frac{r_s + r_f}{r_f}\right)^2$
k_c	Interaction parameter for a given polymer-solvent system (nm^{-1})
ν	Screening parameter
k_1	Constant for a given polymer-solvent system, dependent on the length of a monomer unit and the stiffness of the polymer chain
k	Hydraulic permeability, estimated using a correlation derived by Jackson and James (1986): $k = 0.31 r_f^2 \phi^{-1.17}$
f	Adjusted volume fraction given by: $f = (1 + r_s/r_f)^2 \phi$
λ	$\lambda = r_f/r_s$
a	$a = 3.727 - 2.460\lambda + 0.822\lambda^2$
b	$b = 0.358 + 0.366\lambda - 0.0939\lambda^2$

Johansson's model (Eq. 3), also based on obstruction-scaling theory, views the gel as a collection of cylindrical cells of a given radius (Johansson, Elvingson, & Loefroth, 1991). Each cell contains an infinitely long polymer rod and is filled with solvent.

$$\frac{D}{D_0} = exp\left[-0.84\alpha^{1.09}\right] \tag{3}$$

Tsai and Strieder's obstruction-scaling model (Eq. 4) (Tsai & Strieder, 1985) assumed a random network of overlapping fibers:

$$\frac{D}{D_0} = \left(1 + \frac{2}{3}\alpha\right)^{-1} \tag{4}$$

Johnson, Berk, Jain, and Deen (1996) (Eq. 5) combined the obstruction model of Johansson with the hydrodynamic term of Phillips, Deen, and Brady (1989). The model includes the hydraulic permeability of the medium, which is considered to be a network of straight, rigid fibers with random, three-dimensional orientation.

$$\frac{D}{D_0} = \frac{exp(-0.84\alpha^{1.09})}{1 + \left(\frac{r_s^2}{k}\right)^{1/2} + \frac{1}{3}\frac{r_s^2}{k}} \tag{5}$$

Clague and Phillips (1996) (Eq. 6) combined Tsai and Strieder's obstruction model (Eq. 4) with a hydrodynamic term. The hydrodynamic effects are calculated by taking the solute as a sphere made up of point singularities, and the polymer fibers are accounted for using a numerical version of the slender-body theory.

$$\frac{D}{D_0} = \left(1 + \frac{2}{3}\alpha\right)^{-1} exp\left(-\pi\phi^{0.174\, ln\left(59.6\frac{r_f}{r_s}\right)}\right) \tag{6}$$

Later, Phillips also combined Johansson's obstruction model (Eq. 3) with the hydrodynamic term of Clague and Phillips (Eq. 6), resulting in a model suitable for hindered diffusion of proteins and micelles in hydrogels (Eq. 7) (Phillips, 2000):

$$\frac{D}{D_0} = e^{-0.84 f^{1.09}} e^{-a\phi^b} \tag{7}$$

These diffusion models are based on specific theories, while protein gels have more complex structure than polymer gels. For example, whey protein gels are formed by chains of protein aggregates (Nicolai et al., 2011), while many polymer gels are formed by polymer fibers with simpler structures (Peppas, Huang, Torres-Lugo, Ward, & Zhang, 2000). Therefore, a screening of these models is required to find out the

suitable models for describing the enzyme diffusion in protein gels. Models that have better prediction could suggest the suitable theory for protein diffusion inside a protein network.

3. Material and methods

3.1. Materials

Whey Protein Isolate (WPI) (Bipro, lot no. JE 034–7–440-6) was purchased from Davisco Food International, Inc. (Le Sueur, USA). This batch of WPI was reported to have a protein content of 97.9 g/100 g dry solid. Milli-Q water (resistivity 18.2MΩcm at 25 °C, Merck Millipore, Billerica, USA) was used in all experiments. All other chemicals used were purchased from Sigma Aldrich (St. Louis, USA).

Enhanced green fluorescent protein (EGFP) was produced in-house at Wageningen University & Research, following the method described by Nolles et al. (2015).

3.2. Methods

3.2.1. Gel preparation

Whey protein isolate was dissolved in water or in 0.05 mol/L sodium chloride solution, the gels made from these solutions are denoted as 'WPI gels' and 'WPI-NaCl gels' respectively. The protein weight fractions of the solutions are shown in Table 2, the volume fraction was calculated based on the voluminosity of heat-induced whey protein aggregates (2.3mL g^{-1}, Grácia-Juliá et al. (2008)), the minimum concentration was chosen based on their critical gelation concentration based on preliminary experiments and literature (Ako, Nicolai, Durand, & Brotons, 2009). The solutions were stirred at room temperature for at least 2 h. Afterward, they were centrifuged at 1000 rpm (~ 200 *g* relative centrifugal force) for 10 min to remove any large aggregates and air bubbles. Then they were degassed using 17.50 μm ultrasonic displacement in an ultrasonic bath for 3 min, followed by another centrifugation step (1000 rpm, 10 min). The pH of the WPI solutions was measured to be pH 7.

The focus of the microscope is usually 30 μm above the glass. If using sliced gel sample for the diffusivity measurements, we cannot ensure that the focus is inside the gel rather than the space between the glass and the gel. Therefore, the gels for fluorescence correlation spectroscopy (FCS) were prepared differently: 200 μL of protein solution was pipetted into each well of a μ-Slide 8-well chambered glass slide (ibidi, Martinsried, Germany). The system was covered and heated for 30 min 90 °C in a hot-air oven. The system was cooled to room temperature and stored at 4 °C. The thickness of the gel layer was 1–2 mm. FCS measurements were performed within 2 to 3 days.

For texture analysis, the gels were prepared by pouring the protein solution into Teflon tubes of 2 cm diameter. The Teflon tubes were then heated at 90 °C in a water bath while rotating at 30 rpm for 30 min. Afterward, the tubes were immediately cooled in ice water and stored at 4 °C. Texture analysis was performed within 2 to 4 days. All measurements were performed at 20 °C.

3.2.2. Fluorescence correlation spectroscopy

Twenty μL of 3.2 μM EGFP solution was pipetted onto the wells of the eight-well plate containing WPI gels. The samples were stored at 4 °C for approximately 20 h before they were measured, to allow the EGFP to disperse homogeneously throughout the system.

The principles and practice of FCS have been explained in the previous paper of the authors (Luo et al., 2017), only the experimental details are described here. FCS was performed on a confocal microscope (Leica TCS SP8, Leica, Microsystem, Wetzlar, Germany). The microscope was equipped with a 63 × 1.20 NA water immersion objective and a supercontinuum white light laser, which emits a continuous spectrum from 470 to 670 nm. EGFP was excited at wavelength 488 nm at a pulsed frequency of 80 MHz. The fluorescence intensity was recorded through a 70 μm pinhole using a 495 nm to 525 nm spectral filter. The fluorescence was recorded via the internal hybrid detector, which was coupled to a PicoHarp 300 TCSPC module (PicoQuant GmbH, Berlin, Germany). Every gel was measured 10 times for 30 s each. Experiments were repeated 3 times at 20 °C and neutral pH, due to the pH-dependency of the used fluorophore. The focal position of the gel in the well was chosen such that the number of fluorescent molecules in the confocal volume at any given time was lower than 10. A blank gel without EGFP was measured to check for noise from the gel. Rhodamine 110 ($D = 4.3 \times 10^{-10} m^2 s^{-1}$ at 20 °C) was used to calibrate the setup. At each calibration, diffusion times between 20 μs and 25 μs and a structural parameter between 5.2 and 6.6 were obtained, resulting in confocal volumes of approximately 0.2 fL.

Fluorescence Fluctuation Spectroscopy software (FFS data processor version 2.3 from Scientific Software Technologies Software Centre, Belarus) was used to fit the fluctuation data to a diffusion model that includes the triplet state of the fluorophore. Ten measurements of one sample were fitted by a global analysis based on the Marquardt-Levenberg nonlinear least-squares method. The goodness of fit was confirmed by the straightness of the weighted residuals and low chi-square values. The confidence intervals of the recovered parameters were calculated by the exhaustive search method. Those procedures were all performed within the software, more details have been described by Skakun, Digris, and Apanasovich (2014).

The hydrodynamic radius of EGFP R_h, were calculated using the Stokes-Einstein equation:

$$R_h = \frac{kT}{6\pi\eta D} \tag{8}$$

where k is the Boltzmann constant, T is the absolute temperature, and η is the viscosity of the solvent.

3.2.3. Texture analysis

To determine the compressive elastic modulus of the protein gels, a texture analyzer (type 5564, Instron, MA, USA) was used. Cylindrical gel samples (diameter 20 mm and height 20 mm) were compressed to 25% of their original height at a rate of 30 mm/min using a 2000 N load cell. The compressional extension and load were logged during the experiment to determine the elastic modulus (Pa):

$$E = \frac{Stress}{Strain} = \frac{F/A_0}{dL/L_0} \tag{9}$$

where F is the load, A_0 is the initial area of the surface where the force of compression is applied, dL is the extension and L_0 is the initial height of the sample. The experiments were repeated at least three times per sample composition.

We calculated M_c (Da), defined as the number-average molecular weight between cross-links Peppas et al. (2000), based on the elastic contribution of the Flory-Rehner model (van der Sman, 2012):

$$M_c = \frac{\rho_s RT}{E} \tag{10}$$

where E is the elastic modulus, R is the gas constant, T is the temperature, ρ_s is the density of the polymer ($1421\,kg\,m^{-3}$, Papiz et al. (1986)). M_c can be considered as the inverse of crosslink density.

Table 2
The weight and volume fraction of WPI gels and WPI-NaCl gels used. WPI-NaCl gels were prepared with 0.05 M NaCl.

WPI gel (wt%)	10	13.3	15	16.7	18.3	20
Volume fraction (−)	0.230	0.306	0.345	0.384	0.421	0.460
WPI-NaCl gel (wt%)	5	10	12.5	15	19.2	20
Volume fraction (−)	0.115	0.230	0.288	0.345	0.442	0.460

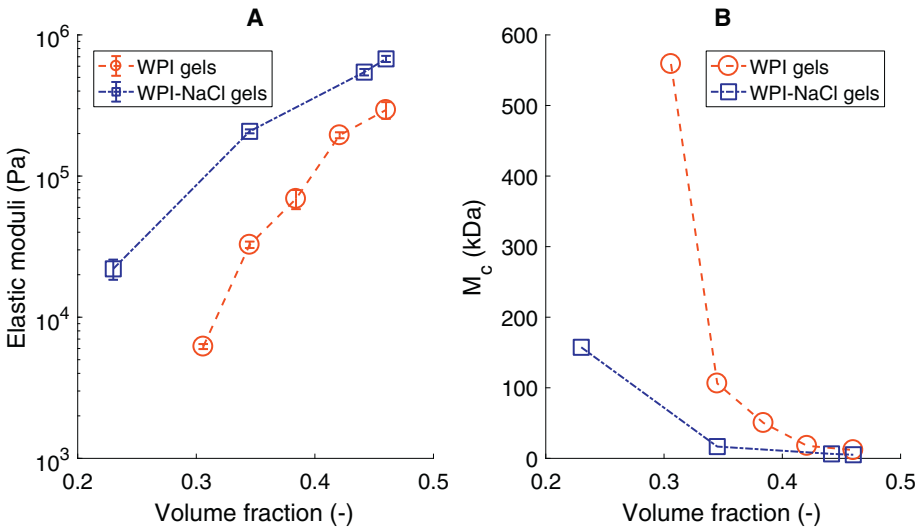

Fig. 1. The elastic moduli (A) and M_c (B) of WPI gels (red circles) and WPI-NaCl gels (blue squares). Each data point is the average of 3 experiments, error bars are the standard deviations. M_c, the number-average molecular weight between cross-links, is the inverse of the crosslinking density. It is calculated based on the elastic contribution of the Flory-Rehner model (Eq. 10). The dashed lines are guides for the eye. (For interpretation of the references to colour in this figure legend, the reader is referred to the web version of this article.)

3.2.4. Modeling

The models for diffusion in hydrogels were fitted to the measured diffusion coefficients using Matlab R2015b (MathWorks, Natick, USA). Model fitting was done using the nonlinear fitting function *lsqcurvefit* that solves fitting problems using a least-squares approach. The algorithm used was the trust-region-reflective method. The accuracy of the resulting fit was analyzed by determining the coefficient of determination of the fit using the *resnorm* option of *lsqcurvefit*. The function *nlparci* was used to extract the 95% confidence interval of the parameters out of the Jacobian matrix.

4. Results and discussion

4.1. Texture analysis

The elastic moduli of the protein gels are reported in Fig. 1A. The WPI gels of 10 wt% and 11.7 wt% and the 5 wt% WPI-NaCl gel behaved like viscous semi-fluids, thus were unfit for elasticity measurements. The crosslinking density, found with the Flory-Rehner equation, is inversely proportional to the elastic modulus (Eq. 10) and is shown in Fig. 1B. It shows that the WPI-NaCl gels are more densely cross-linked, which agrees with the observation that the protein aggregates at higher ionic strengths are more strongly branched (Nicolai et al., 2011).

The crosslinking density of the gels will be compared with their effect on diffusivity in the following section. One should bear in mind that the gel samples for texture analysis and FCS measurements were prepared with the same temperature but a slightly different method. This may have some impact on the microstructure.

4.2. Diffusivity experiments

4.2.1. Report on diffusivity data

The diffusivity of EGFP in water and in gels was assessed using FCS. The autocorrelation curves obtained via FCS were fitted with a one-component model resulting in a good fit, yielding a diffusion coefficient of EGFP in water of $1.3 \times 10^{-10} m^2 s^{-1}$. The diffusivity reduction (D/D_0) of EGFP in both the WPI and WPI-NaCl gels were calculated and reported in Fig. 2. As expected, the diffusivity in both types of gels decreases as the WPI concentration increases. While the two types of gels had distinctive trends in the change of their elastic moduli (Fig. 1A), they do not show any significant differences in their reduction in diffusivity. Therefore, although both elasticity and diffusivity are related to the gel microstructure, these two properties are not directly correlated. We see that the volume fraction of the protein gel is the main determinant of the diffusivity reduction, and we expect that

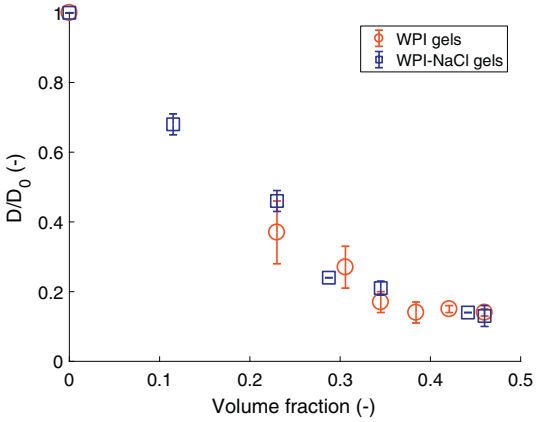

Fig. 2. Diffusivity reduction (D/D_0) of enhanced green fluorescent protein in WPI gels (red circles) and WPI-NaCl gels (blue squares). Each data point is the average of 2 or more experiments, error bars are the standard deviations. The dashed lines are guides for the eye. (For interpretation of the references to colour in this figure legend, the reader is referred to the web version of this article.)

the elastic modulus will be also be determined by the exact microstructure of the gel.

This does not mean that the gel microstructure has no influence on the diffusion related properties. The diffusion of pepsin into the gel is a necessary first step in the gastric digestion of protein gels. Guo et al. found that food gels that have the same protein volume fraction but different strength, do differ in their gastric disintegration kinetics (Guo et al., 2015). Although the microstructure of the gels (elasticity or fracture strength) may not determine the diffusivity reduction in the gels, it is correlated with other factors that contribute to the ultimate disintegration of the gel.

4.2.2. Model fitting and analysis

The models discussed in the theory section (Eq. 1–7) are examined using the experimental diffusivity data. In the fitting process, the radius of EGFP r_s (1.65 nm) is calculated from the measured diffusion coefficient in water, using the Stokes-Einstein equation (Eq. 8); the radius of the polymer fiber and the other unknown constants are used as fitted parameters. All the fitted parameters are shown in Table 3.

In Cukier's model (Eq. 1), the screening parameter v has been shown to vary in different regimes of concentrations. By definition, in the dilute regime, polymer chains move independently; in the semi-dilute

Table 3
The fitted parameters of the models. The uncertainty are the 95% confidence intervals of the fit.

Model	Matrices	Fitted parameter	Value	R^2	SSR
Cukier 0.75	WPI gel	k_c (nm^{-1})	2.11 ± 0.23	0.987	0.008
	WPI-NaCl gel		1.83 ± 0.43	0.950	0.038
Cukier 1	WPI gel	k_c (nm^{-1})	2.77 ± 0.22	0.994	0.004
	WPI-NaCl gel		2.51 ± 0.38	0.980	0.015
Ogston	WPI gel	r_f (nm)	1.00 ± 0.25	0.974	0.016
	WPI-NaCl gel		1.39 ± 0.84	0.885	0.081
Johansson	WPI gel	r_f (nm)	1.29 ± 0.08	0.994	0.003
	WPI-NaCl gel		1.39 ± 0.15	0.985	0.011
Tsai	WPI gel	r_f (nm)	0.55 ± 0.11	0.976	0.015
	WPI-NaCl gel		0.69 ± 0.23	0.926	0.057
Johnson	WPI gel	r_f (nm)	0.05 ± 0.06	0.921	0.046
	WPI-NaCl gel		0.24 ± 0.32	0.757	0.179
Clague	WPI gel	r_f (nm)	4.73 ± 1.71	0.992	0.005
	WPI-NaCl gel		8.23 ± 5.47	0.979	0.017
Phillips	WPI gel	r_f (nm)	3.02 ± 11.2	0.990	0.007
	WPI-NaCl gel		2.99 ± 18.06	0.952	0.048

regime, polymer chains start to overlap; and in the concentrated regime, diffusion is dominated by polymer friction. Cukier found an exponent of 0.5 for small solutes in semi-dilute polymer solutions and slightly cross-linked gels (Cukier, 1984). Freed and Edwards (1974) obtained an exponent of 1 for polymer chains in a dense polymer solution without entanglements. De Gennes found an exponent of 0.75 in a system of long flexible chains in good solvents (De Gennes, 1976). Thévenot et al. applied Cukier's model with the exponent of 0.75 to the diffusion of labelled pepsin in casein rennet gels and found good fitting description (Thévenot et al., 2017). To determine which screening factor should be used in the EGFP-WPI gel system, we evaluated the model with both v = 0.75 and v = 1 (Later denoted as Cukier 0.75 and Cukier 1). The model predictions are illustrated in Fig. 3A/B, the fitted parameters and the goodness of fit are listed in Table 3.

Overall, the Cukier's model describes the diffusivity in our system well. In comparison, using an exponent of 1 yields better fit than using 0.75. Since we studied the whey protein gels above the critical gelation concentration, the gels are densely cross-linked which fall in the concentrated regime. The fitted interaction parameter k_c differs slightly between WPI gels and WPI-NaCl gels, however, there is a strong overlap between their 95% confidence intervals.

In the other models, we used r_f as the fitted parameter. Among them, Johansson's model and Clague-Phillips' model yielded the best fit, with low SSR, high R^2. These two models are shown in Fig. 3 C/D as the examples. The typical β-lactoglobulin primary aggregates radius is 5 nm, observed with cryo-TEM (Pouzot et al., 2005). In Johansson's model, the fitted polymer radii r_f are 1.29 nm and 1.39 nm, which are smaller than the protein aggregate radius. Ogston's model and Tsai-Strieder's model also yielded reasonable fit while the fitted polymer radii are small. The diffusivity reduction may be affected by more than the hydrodynamic or obstruction hindrance that is described in the models, and these effects were reflected in the small r_f in the fitting. In the Phillips' model, the confidence intervals are very large which indicate that there is no strong correlation between the fitted parameter and experimental data.

We tested whether the different models can predict the diffusivity of pepsin in WPI gels using the parameters yielded from the EGFP. Cukier 1, Johansson's and Clague-Phillips' models were chosen for the prediction. The experimentally determined diffusion coefficients of Alexa633-labelled pepsin from our previous study (Luo et al., 2017) were used. In the models, the hydrodynamic radius of the Alexa633-labelled pepsin (2.9 nm) was used, while for other parameters we used the values that were obtained with EGFP diffusion in WPI gels. The prediction is shown in Table 4. Cukier's model predicted far lower diffusion coefficients for both gel types. This may indicate that interaction parameter k_c is not only dependent on the polymer-solvent system but also the solute's interaction with the polymer, for example, due to different charge or charge distribution over the different

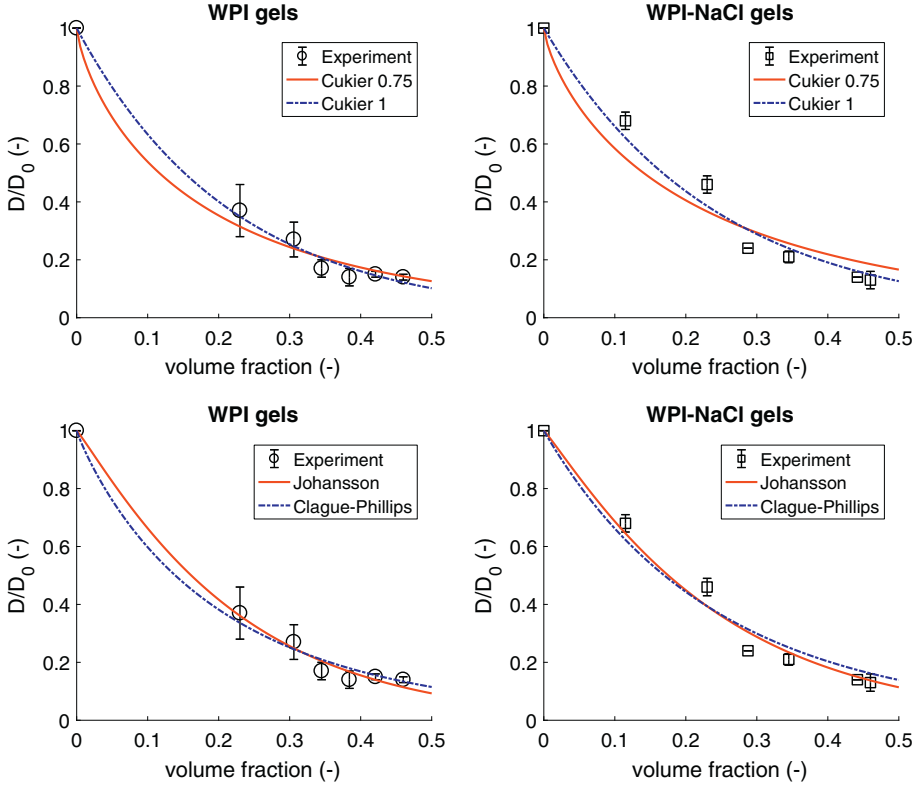

Fig. 3. Diffusivity reduction (D/D_0) of EGFP in WPI gels (A/C) and WPI-NaCl gels (B/D) and the model predictions. The black circles and squares are the average of 3 or 4 experimental data measured by fluorescence correlation spectroscopy, error bars are their standard deviation. The lines are the model predictions.

Table 4
Experimental data and model predictions of diffusivity reduction (D/D_0) of Alexa 633 labelled pepsin, experimental data is taken from Luo et al. (2017).

Gel type	D/D_0, experimental	Cukier 1	Clague	Johansson
WPI gel 15 wt%	0.26	0.063	0.163	0.032
WPI gel 20 wt%	0.16	0.025	0.102	0.0091

proteins. Johansson's model also underestimated the diffusion coefficients, while Clague's model predicted values that are about 60% of the experiment data, providing the closest prediction among the models. The small polymer fiber radii used in the Johansson's caused the prediction to be very sensitive to the change of the solute radius r_s. The prediction is too low in all cases, indicating that pepsin is anomalously mobile relative to EGFP in WPI gels, even though the molecular weights are similar, with pepsin slightly larger than EGFP, and EGFP is a very compact molecule compared to other proteins.

The different diffusion behavior of pepsin may be related to a number of effects, as all these models presume to a specific interaction between the diffusant and the matrix.

The first possible interaction is the electrostatic interaction. Kang et al. studied the diffusion of apoferritin (diameter 12.8 nm) in bacteriophage fd (a rod-like virus with contour length of 880 nm and bare diameter of 6.6 nm) solution (Kang, Wilk, Patkowski, & Dhont, 2007). They found that the electrostatic interactions strongly alter the diffusional behavior of apoferritin. Likewise, both EGFP and whey proteins are charged at neutral pH, as well as pepsin. Pepsin, having a very low isoelectric point (IEP), has around 20 negatively charged groups, and will be quite negatively charged at neutral pH. EGFP, in contrast, has a much higher IEP and is only slightly negatively charged at neutral pH. One would expect that pepsin, being more strongly charged, would have less accessible volume in the WPI gel network, especially in more concentrated gels. However, we see that the experimental diffusivities of pepsin are significantly higher than would be expected based on the diffusivity of EGFP in WPI gels.

A second interaction is binding. Pepsin as an enzyme naturally binds to protein, which also negatively affects its diffusivity. We previously observed that a part of the pepsin diffuses slower than the expected reduction by the whey protein gel network even at neutral pH where pepsin's activity is very lowis (Luo et al., 2017). Fadda et al. found anomalously slow diffusion of thermolysin in gelatin gels due to the enzyme-substrate interaction, and the time that the enzyme is trapped on the gel is related to the enzyme kinetics constants. K_m determines the proportion of enzyme that is trapped in the enzyme substrate, and k_{cat} offers an estimate of the elementary trapping time. However, also this aspect would imply a lower diffusion rate for pepsin than for EGFP. One may argue that the hydrolytic action of pepsin may lead to a greater degree of freedom for pepsin to diffuse in a gel matrix; however, our measurements with pepsin were made at neutral pH, and pepsin is not catalytically active at this condition.

5. Conclusions

We investigated the diffusivity of EGFP, as a model for pepsin, in two types of whey protein gels with varied concentrations. The diffusion rates of EGFP decreased dramatically at higher concentrations of whey protein in the gel. Two types of whey protein gels, made with different ionic strength had different elastic moduli at the same protein concentration, but the elastic moduli cannot be directly correlated to the diffusivity reduction.

Cukier's hydrodynamic model yielded the best description, but the parameter k_c cannot directly reflect the geometry of the gel matrix; and it varies among different gel matrices. In contrast, Clague's, Johansson's and Phillips' models require only basic structural information such as the radius of the polymer fiber (r_f) and the radius of the solute (r_s).

Surprisingly, the EGFP diffusivity measurements predicted significantly lower diffusivities for pepsin, than was found with pepsin itself. In the translation from EGFP to pepsin, we need to include the different electrostatic interaction and possible enzyme-substrate interaction; however, both effects cannot explain the less reduced diffusivity of pepsin in WPI gels compared to that of EGFP.

We conclude that while the hydrodynamic models give good descriptions, they are clearly too simple for a full physical understanding of diffusion of a protein in a protein gel, and that the translation from one diffusant to another may involve several types of interactions.

References

Ako, K., Nicolai, T., Durand, D., & Brotons, G. (2009). Micro-phase separation explains the abrupt structural change of denatured globular protein gels on varying the ionic strength or the pH. *Soft Matter, 5*, 4033–4041. https://doi.org/10.1039/B906860K.

Amsden, B. (1998). Solute Diffusion within Hydrogels. Mechanisms and Models. *Macromolecules, 31*, 8382–8395. https://doi.org/10.1021/ma980765f.

Aymard, P., Gimel, J. C., Nicolai, T., & Durand, D. (1996). Experimental evidence for a two-step process in the aggregation of *β*-lactoglobulin at pH 7. *Journal de Chimie Physique, 93*, 987–997. https://doi.org/10.1051/jcp/1996930987.

Bornhorst, G. M., & Singh, R. P. (2014). Gastric Digestion In Vivo and In Vitro: How the Structural Aspects of Food Influence the Digestion Process. *Annual Review of Food Science and Technology, 5*, 111–132. https://doi.org/10.1146/annurev-food-030713-092346.

Clague, D. S., & Phillips, R. J. (1996). Hindered diffusion of spherical macromolecules through dilute fibrous media. *Physics of Fluids, 8*, 1720–1731. https://doi.org/10.1063/1.868884.

Cukier, R. I. (1984). Diffusion of Brownian spheres in semidilute polymer solutions. *Macromolecules, 17*, 252–255. https://doi.org/10.1021/ma00132a023.

De Gennes, P. G. (1976). Dynamics of Entangled Polymer Solutions. I. The Rouse Model. *Macromolecules, 9*, 587–593. https://doi.org/10.1021/ma60052a011.

Floury, J., Bianchi, T., Thévenot, J., Dupont, D., Jamme, F., Lutton, E., ... Le Feunteun, S. (2018). Exploring the breakdown of dairy protein gels during in vitro gastric digestion using time-lapse synchrotron deep-UV fluorescence microscopy. *Food Chemistry, 239*, 898–910. https://doi.org/10.1016/j.foodchem.2017.07.023.

Freed, K. F., & Edwards, S. F. (1974). Polymer viscosity in concentrated solutions. *The Journal of Chemical Physics, 61*, 3626–3633. https://doi.org/10.1063/1.1682545.

Grácia-Juliá, A., René, M., Cortés-Muñoz, M., Picart, L., López-Pedemonte, T., Chevalier, D., & Dumay, E. (2008). Effect of dynamic high pressure on whey protein aggregation: A comparison with the effect of continuous shorttime thermal treatments. *Food Hydrocolloids, 22*, 1014–1032. https://doi.org/10.1016/j.foodhyd.2007.05.017.

Guo, Q., Ye, A., Lad, M., Ferrua, M., Dalgleish, D., & Singh, H. (2015). Disintegration kinetics of food gels during gastric digestion and its role on gastric emptying: An in vitro analysis. *Food & Function, 6*, 756–764. https://doi.org/10.1039/C4F000700J.

Jackson, G. W., & James, D. F. (1986). The permeability of fibrous porous media. *The Canadian Journal of Chemical Engineering, 64*, 364–374. https://doi.org/10.1002/cjce.5450640302.

Johansson, L., Elvingson, C., & Loefroth, J. E. (1991). Diffusion and interaction in gels and solutions. 3. Theoretical results on the obstruction effect. *Macromolecules, 24*, 6024–6029. https://doi.org/10.1021/ma00022a019.

Johnson, E. M., Berk, D. A., Jain, R. K., & Deen, W. M. (1996). Hindered diffusion in agarose gels: Test of effective medium model. *Biophysical journal, 70*, 1017–1023.

Kang, K., Wilk, A., Patkowski, A., & Dhont, J. K. (2007). Diffusion of spheres in isotropic and nematic networks of rods: Electrostatic interactions and hydrodynamic screening. *The Journal of chemical physics, 126*, 214–501.

Luo, Q., Boom, R. M., & Janssen, A. E. M. (2015). *Digestion of protein and protein gels in simulated gastric environment. LWT - Food Science and Technology. 63*, 161–168. https://doi.org/10.1016/j.lwt.2015.03.087.

Luo, Q., Borst, J. W., Westphal, A. H., Boom, R. M., & Janssen, A. E. M. (2017). Pepsin diffusivity in whey protein gels and its effect on gastric digestion. *Food Hydrocolloids, 66*, 318–325. https://doi.org/10.1016/j.foodhyd.2016.11.046.

Masaro, L., & Zhu, X. X. (1999). Physical models of diffusion for polymer solutions, gels and solids. *Progress in Polymer Science, 24*, 731–775. https://doi.org/10.1016/S0079-6700(99)00016-7.

Nicolai, T., Britten, M., & Schmitt, C. (2011). *β*-Lactoglobulin and WPI aggregates: Formation, structure and applications. *Food Hydrocolloids, 25*, 1945–1962. https://doi.org/10.1016/j.foodhyd.2011.02.006.

Nolles, A., Westphal, A. H., de Hoop, J. A., Fokkink, R. G., Kleijn, J. M., van Berkel, W. J. H., & Borst, J. W. (2015). Encapsulation of GFP in Complex Coacervate Core Micelles. *Biomacromolecules, 16*, 1542–1549. https://doi.org/10.1021/acs.biomac.5b00092.

Ogston, A. G., Preston, B. N., & Wells, J. D. (1973). On the Transport of Compact Particles Through Solutions of Chain-Polymers. *Proceedings of the Royal Society of London. A. Mathematical and Physical Sciences, 333*, 297–316. https://doi.org/10.1098/rspa.1973.0064.

Ormo, M., Cubitt, A. B., Kallio, K., Gross, L. A., Tsien, R. Y., & Remington, S. J. (1996). Crystal Structure of the *Aequorea victoria* Green Fluorescent Protein. *Science, 273*, 1392–1395. https://doi.org/10.1126/science.273.5280.1392.

Papiz, M., Sawyer, L., Eliopoulos, E., North, A., Findlay, J., Sivaprasadarao, R., ... Kraulis, P. (1986). The structure of b- lactoglobulin and its similarity to plasma retinol-binding protein. *Nature, 324*, 383–385.

Peppas, N. A., Huang, Y., Torres-Lugo, M., Ward, J. H., & Zhang, J. (2000).

Physicochemical Foundations and Structural Design of Hydrogels in Medicine and Biology. *Annual Review of Biomedical Engineering, 2*, 9–29. https://doi.org/10.1146/annurev.bioeng.2.1.9.

Phillips, R. J. (2000). A hydrodynamic model for hindered diffusion of proteins and micelles in hydrogels. *Biophysical Journal, 79*, 3350–3353.

Phillips, R. J., Deen, W. M., & Brady, J. F. (1989). Hindered transport of spherical macromolecules in fibrous membranes and gels. *AIChE journal, 35*, 1761–1769.

Pouzot, M., Nicolai, T., Visschers, R. W., & Weijers, M. (2005). X-ray and light scattering study of the structure of large protein aggregates at neutral pH. *Food Hydrocolloids, 19*, 231–238. https://doi.org/10.1016/j.foodhyd.2004.06.003.

Sielecki, A. R., Fedorov, A. A., Boodhoo, A., Andreeva, N. S., & James, M. N. (1989). Molecular and crystal structures of monoclinic porcine pepsin refined at 1.8 A resolution. *J.Mol.Biol. 214*, 143–170. https://doi.org/10.1016/0022-2836(90)90153-D.

Singh, H., Ye, A., & Ferrua, M. J. (2015). Aspects of food structures in the digestive tract. *Current Opinion in Food Science, 3*, 85–93. https://doi.org/10.1016/j.cofs.2015.06.007.

Skakun, V., Digris, A., & Apanasovich, V. (2014). Global Analysis of Autocorrelation Functions and Photon Counting Distributions in Fluorescence Fluctuation Spectroscopy. In Y. Engelborghs, & A. J. W. G. Visser (Eds.). *Fluorescence Spectroscopy and Microscopy number 1076 in Methods in Molecular Biology* (pp. 719–741). New York: Humana Press.

Thévenot, J., Cauty, C., Legland, D., Dupont, D., & Floury, J. (2017). Pepsin diffusion in dairy gels depends on casein concentration and microstructure. *Food Chemistry, 223*, 54–61. https://doi.org/10.1016/j.foodchem.2016.12.014.

Tsai, D. S., & Strieder, W. (1985). Radiation across a spherical cavity having both specular and diffuse reflectance components. *Chemical engineering science, 40*, 170–173.

van der Sman, R. G. M. (2012). Thermodynamics of meat proteins. *Food Hydrocolloids, 27*, 529–535. https://doi.org/10.1016/j.foodhyd.2011.08.016.